

**SYNTHESIS, BIODISTRIBUTION AND QSAR STUDIES
OF FIVE Tc-99M LABELED NOVEL N₃S PSEUDO-PEPTIDE COMPLEXES**

Hua-bei Zhang^{**}, Hai-hong Ye[†], Ya-ling Zhang[†], Xuefang Zheng[†], Jian-sheng Han[†],
Hua Li[†], Chun-ping Liu[†]

[†]Department of Chemistry, Beijing Normal University, Beijing 100875, China

[‡]Liaoning Key Laboratory of Bio-organic Chemistry, Dalian University, Dalian
116622, China

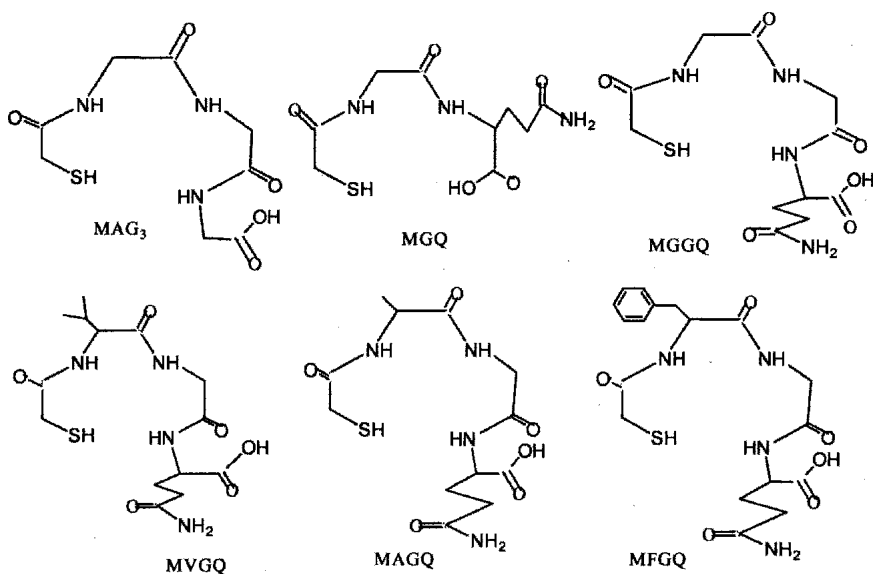
Abstract. Five novel N₃S pseudo-peptide chelators derived from mercaptoacetic acid have been synthesized and characterized based on the spectroscopic data. All the chelators were labeled with Technetium-99m to evaluate their biological activities. Investigations of their biodistribution in mice showed all five pseudo-peptide chelators (MGQ, MGGQ, MAGQ, MVGQ, MFGQ) are rapidly cleared from blood, mainly through renal clearance. ^{99m}Tc-MGGQ and ^{99m}Tc-MVGQ had high kidney uptake, quick blood clearance and high activity ratios of kidney to blood, thus showing potential application as renal imaging agents. Quantitative structure-activity relationship studies were performed. Linear regression analysis between the logarithm of renal uptake value (log%ID) and the parameters obtained from the ZINDO/1 method elicited several equations that possessed certain predictive qualities, and may play a direct part in drug design and synthesis.

Technetium-99m (^{99m}Tc) is one of the most desirable radioactive nuclides in diagnostic nuclear medicine for external imaging, due to the emission of gamma rays at an optimal energy (140keV), suitable half-life, and availability from ⁹⁹Mo-^{99m}Tc generator systems. Technetium-99m labeled imaging agents play an important role in

* Corresponding author. Tel: +86-10-62205194; fax: +86-10-6220-0567 E-mail address:
hbzhang@bnu.edu.cn

nuclear medicine. Since polypeptides are important components of the plant and animal kingdom, and that they tend to possess significant and complicated biological activities, we were interested in evaluating novel peptides. Studies of Tc-99m-labeled small peptides or pseudo-peptides as imaging agents have been a focal point for radio-pharmaceuticals due to their low toxicity, target-specificity, broad application and promising potential of application¹⁻⁵. In 1986, Fritzberg et al. successfully developed the first peptide renal imaging agent (^{99m}Tc-MAG₃). Much progress has been made in the past decade in thrombus imaging agents⁶⁻⁷ as well as tumor imaging agents⁸⁻⁹. At present, the design and synthesis of Tc-99m-labeled radiopharmaceuticals mainly focus on the modification and optimization of a known biologically active ligand structure, with an emphasis to improve the imaging quality. For example, in 1984, ^{99m}Tc-d,l-HMPAO became the first brain perfusion imaging agent authorized by Food and Drug Administration (FDA) in the U.S.¹⁰. This was identified from more than one hundred new compounds that were derived from ^{99m}Tc-PnAO. In 1988, Cheesman et al. reported ^{99m}Tc-ECD, which was another brain perfusion imaging agent developed from ^{99m}Tc-BAT¹¹. Therefore, it seems of interest to introduce functional groups that alter the fundamental structure of MAG₃ (Scheme 1) and may yield new radio-pharmaceuticals with high affinity for organic tissues.

Research in renal imaging agents has also been achieved¹²⁻¹⁴. The present work, based on previous research in our lab¹⁵⁻¹⁶, involved five new pseudo-peptide chelators (Scheme 1) which were designed and synthesized with mercaptoacetic acid as the primary material for the novel ^{99m}Tc-labeled renal imaging agents. We introduced hydrophobic groups such as isopropyl, methyl and propionamide to the lead compound, MAG₃, and successfully obtained two target compounds MGGQ and MVGQ, respectively (Scheme 2). Both complexes labeled by Tc-99m showed potential as renal imaging agents.



Scheme 1. Structure of MAG_3 , MGQ , MGGQ , MVGQ , MAGQ and MFGQ

Chemistry

The protection of the mercapto group was completed according to the method of Capretta et al¹⁷. the yield of compound 2 (colorless crystal) was 93%, m.p 158.4-160.1, IR (cm^{-1}): 3026.9(s), 3054.7(s), 3431.7(s), 1705.4(s), 1594.4(s), 1488.6, 1445.8(m).

The active ester of compounds 2, 4, 5, 6 and 7 were prepared according to the literature method¹⁸. Yield 86%. m.p. 176.4-178.5°C. IR (cm^{-1}): 3060.2, 3028.4, 2930.6, 1811.2, 1782.6, 1738.2, 1594.6, 1490.7, 1445.1, 846.2, 742.9, 699.4.

IR spectra of each showed the characteristic absorption of active esters at 1820 cm^{-1} , 1790 cm^{-1} , and 1740 cm^{-1} , indicating that the reaction had occurred. So the active esters of compounds 4, 5, 6 and 7, without purification, were directly transformed in the similar manner used for synthesizing target compounds 9, 10, 11 and 12.

Synthesis of Compounds 4, 5, 6 and 7

Compound 4 (N-[[[(triphenylmethyl)thio]acetyl]- (9CI), Glycine) : m.p. 166.7-168.1⁰C;
IR (KBr, cm⁻¹): 3420.5(br), 3343.7, 3054.9(m), 2926.4(m), 1732.8, 1621.1, 1539.2,
1448.5, 1445.2, 741.2, 703.4; ¹HNMR(500MHz, DMSO), δ (ppm):
12.55(1H,br,COOH); 8.27(1H,NH); 7.37-7.26(15H,m,Ar); 3.67(2H,d, CH₂);
2.82(2H,s,CH₂).

Compound 5 (N-[[[(triphenylmethyl)thio]acetyl]- (9CI), L-Alanine) : m.p.
101.4-102.5⁰C, IR (KBr, cm⁻¹): 3424.9(br), 3056.1(m), 2928.3, 1727.8, 1623.0,
1529.5, 1489.6, 1448.4, 744.1, 701.1; ¹HNMR(500MHz, DMSO), δ (ppm) :
12.55(1H,br,COOH), 8.27(1H,d,NH), 7.25-7.37(15H,m,Ar), 4.10(1H,m,NCHCO),
2.85(1H,d,SCHCO), 2.80(1H,d,SCHCO), 1.20(3H,d,CH₃).

Compound 6 (N-[[[(triphenylmethyl)thio]acetyl]- (9CI), L-Valine) : m.p.
147.2-149.0⁰C, IR(KBr, cm⁻¹): 3420.5(br), 3056.7, 2961.6, 2929.6, 1738.5, 1637.6,
1535.0, 1488.5, 1444.9, 739.5, 701.0; ¹HNMR(500MHz, DMSO), δ (ppm): 12.62
(1H, br, COOH), 8.20(1H,d,NH), 7.37-7.26 (15H, m, Ar), 4.08 (1H, dd, NCHCO),
2.93(1H,d,SCHCO), 2.86(1H,d,SCHCO), 2.01(1H, m, CH₃CHCH₃), 0.85(6H, d,
CH₃).

Compound 7 (N-[[[(triphenylmethyl)thio]acetyl]- (9CI), L-Phenylalanine): m.p. 129.2-131.9°C, IR (KBr, cm^{-1}): 3440.3(br), 3054.8, 2984, 2927.8, 2850.3, 1705.2, 1626.3, 1594.1, 1488.6, 1445.8, 749.8, 701.5; $^1\text{H-NMR}$ (500MHz, DMSO), δ (ppm): 12.85(1H,br, COOH), 8.34(1H,d,NH), 7.19-7.35(20H,m,Ar), 4.35(1H,m,NCHCO), 3.00(1H,dd,phCH), 2.85(1H,dd,phCH), 2.75(2H,s,SCH₂CO).

Target Ligands

Compound 8 ((N-[[[(triphenylmethyl)thio]acetyl]-L-glycyl- (9CI), L-Glutamine)): m.p. 65.2~67.3°C, IR (KBr, cm^{-1}): 3394.8(br), 3056.6, 2925.8, 1660.5, 1607.4, 1529.7, 744.1 701.3; $^1\text{H-NMR}$ (500 MHz, DMSO), δ (ppm): 12.1(1H,br,COOH), 7.22-7.45(15H,m, Ar), 6.90(1H,br,NH₂), 6.73(1H,br,NH₂), 5.83(1H,br,NH), 5.37(1H,br,NH), 3.16(2H,s,SCH₂), 3.66(2H,dd,NCH₂), 4.37(1H,m,NCH), 1.99(1H,m,NCHCH₂), 2.23(1H,m,NCHCH₂), 2.30(2H,dd,CH₂CONH₂); $^{13}\text{C-NMR}$ (500 MHz, DMSO), δ (ppm): 175.6, 168.2, 143.9, 129.5, 128.2, 127.0, 53.3, 45.3, 43.2, 35.8, 32.1, 28.8.

Compound 9 ((N-[[[(triphenylmethyl)thio]acetyl]-L-glycylglycyl- (9CI), L-Glutamine)): m.p. 88.2~90.5°C, IR (KBr, cm^{-1}): 3384.8 (br), 3056.3, 2923.4, 2852.0, 1658.8, 1531.7, 1444.6, 1397.6, 743.9, 700.6; $^1\text{H-NMR}$ (500 MHz, DMSO), δ (ppm): 12.3(1H,br,COOH), 7.98(1H,br,NH), 7.21-7.43(15H,m,Ar), 6.92(2H,br,NH₂), 5.77(1H,br,NH), 5.32(1H,br,NH), 4.33(1H,m,NHCHCO), 3.94(1H,dd,NCH₂), 3.83(1H,dd,NCH₂), 3.68(2H,dd,NCH₂), 3.14(2H,s,SCH₂), 2.25(2H,m,CH₂CONH₂), 2.18(1H,m,CH₂CH₂CONH₂), 1.97(1H,m,CH₂CH₂CONH₂); $^{13}\text{C-NMR}$ (500 MHz, DMSO), δ (ppm): 176.0, 169.5, 168.8, 143.9, 130.1, 129.3, 128.1, 54.2, 45.4, 44.9, 35.8.

Compound 10 (N-[[[(triphenylmethyl)thio]acetyl]-L-alanylglycyl- (9CI), L-Glutamine): m.p. 93.8~95.4°C, IR (KBr, cm^{-1}): 3396.7 (br), 3056.3, 2974.8, 2934.4, 1658.9, 1607.3, 1515.6, 1445.5, 1386.8, 744.3, 701.3; $^1\text{H-NMR}$ (500 MHz,

DMSO), δ (ppm): 11.8(1H,br,COOH), 7.24-7.45(15H,m,Ar), 7.13(1H,br,NH₂), 7.07(1H,br,NH₂), 6.99(1H,br,NH), 6.72(1H,br,NH), 5.62(1H,br,NH), 4.29(1H,m,NCHCO), 4.20(1H,m,NCHCO), 3.88(2H,dd,NHCH₂), 3.16(2H,s,SCH₂), 2.27(2H,m,CH₂CONH₂), 2.20(1H,m,CH₂CH₂CONH₂), 1.98(1H,m,CH₂CH₂CONH₂), 1.24(3H,d,CH₃).

Compound 11(N-[[[(triphenylmethyl)thio]acetyl]-L-valylglycyl]- (9CI), L-Glutamine): m.p. 113.3~116.2⁰C, IR (KBr, cm⁻¹): 3382.2(br), 3056.1, 2967.9, 1657.7, 1605.6, 1538.8, 743.7, 701.1; ¹H-NMR(500 MHz, DMSO), δ (ppm): 7.23-7.40(15H,m,Ar), 0.86-0.90(6H,dd,CH₃), 1.96(1H,m,CH), 4.29(1H,m,CH), 4.14(1H,dd,CH), 1.18(2H,m,CH₂), 2.85(2H,s,SCH₂), 3.92(2H,m,NCH₂), 3.08(2H,m,NCH₂), 7.09(1H,br,NH), 6.98(1H,br,NH), 6.77(1H,br,NH), 5.72(2H,d,NH₂), 12.31(H, b, COOH); ¹³C-NMR (500 MHz, DMSO): δ (ppm): 176.1, 175.9, 170.9, 168.6, 168.5, 168.3, 168.2, 144.1, 129.6, 128.1, 127.1, 67.8, 58.8, 58.7, 54.0, 45.6, 43.0, 32.6, 30.9, 29.6, 19.2, 18.2.

Compound 12 ((N-[[[(triphenylmethyl)thio]acetyl]-L-phenylalanyl]glycyl]- (9CI), L-Glutamine): m.p. 89.2~92.6⁰C, IR(KBr,cm⁻¹): 3377.5 (br), 3057.0, 2937.6, 1658.5, 1602.5, 1521.5, 1444.3, 1396.2, 743.8, 700.7; ¹HNMR(500MHz, DMSO), δ (ppm): 12.65(1H,br,COOH), 8.41(2H,br,CONH₂), 8.21(1H,br,NH), 7.60(1H,br,NH), 6.65(1H,br,NH), 7.15-7.34(20H,m,Ar), 4.44(1H,m,NCHCO), 3.91(1H,m,NCHCO), 3.70(2H,NCH₂CO), 3.04(1H,dd,phCH), 2.85(1H,dd,phCH), 2.75(2H,SCH₂CO), 2.02(2H,m,CH₂CONH₂), 1.74(2H,m,CH₂CH₂CONH₂); ¹³CNMR(500MHz, DMSO), δ (ppm): 174.90, 173.06, 171.76, 168.05, 167.72, 129.63, 128.54, 127.24, 126.68, 54.78, 46.03, 42.78, 37.92, 36.41, 32.31, 22.14.

Biodistribution

Organic distribution of ^{99m}Tc-labeled complexes was determined in female Kun Ming mice (20 ± 2g) by injecting 0.1mL ^{99m}Tc-complex solutions which we obtained adapting the method mentioned above via tail vein into rats (activity range from

0.56MBq to 0.74MBq). Tissues and organs including heart, brain, liver, lung, kidney, spleen and blood, were excised from three mice sacrificed by decapitation, bled from the neck and dissected at 0.5min, 2min, 5min, 15min, 30min, 60min post injection. The tissues and organs were then weighed. The percent of injected dose (%ID) in each tissue was calculated.

All of the compounds have high kidney uptake and quick blood clearance (Fig 1, Fig 2). From Table 4, ^{99m}Tc -MVGQ had high kidney uptake and quick blood clearance. The uptake value of ^{99m}Tc -MVGQ in kidney was 43.66%ID/g at 2 min post injection (p.i.), as well as 2.64%/g at 60 min p.i. and the lifetime of blood clearance was below 5 min. It's noted that that the corresponding activity ratios of kidney to other organs were high (Table 7). The activity ratio of kidney to blood of ^{99m}Tc -MVGQ was 4.16 at 2 min and 5.75 at 5min, but 4.80 at 15 min and 1.17 at 60 min. While that of ^{99m}Tc -MAG₃ was 5.43 at 15 min and 3.28 at 60 min, indicating that the activity ratio of kidney to blood of ^{99m}Tc -MVGQ was lower than that of ^{99m}Tc -MAG₃. It shows that ^{99m}Tc -MVGQ has potential application as a renal function imaging agent.

Table 2 shows the biodistribution results of ^{99m}Tc -MGGQ. From Table ^{99m}Tc -MGGQ shows similar biological activity as ^{99m}Tc -MAG₃. ^{99m}Tc -MGGQ possessed high kidney uptake (24.77%ID/g) and the activity ratio of kidney to blood (about 2) remained relatively stable. Its activity ratio of kidney to liver was high (5.53 at 2 min and 3.76 at 5 min). ^{99m}Tc -MGGQ also showed quick clearance in blood, liver and lung. The residual dosage in these tissues was very low. Based on this, ^{99m}Tc -MGGQ remains an excellent candidate for renal dynamic imaging.

Table 1 Distribution of ^{99m}Tc - MGQ in mice (%ID/g, n=3)

t/min	Heart	Liver	Spleen	Lung	Kidney	Brain	Blood
0.5	4.65±0.56	5.86±0.96	3.71±0.07	11.19±1.1	25.95±5.3	0.55±0.04	34.91±4.8
2	3.44±0.60	5.80±0.28	2.50±0.55	8.38±0.67	20.29±4.21	0.59±0.12	20.15±2.3
5	2.15±0.31	7.17±0.92	2.09±0.17	5.57±1.08	17.06±2.89	0.31±0.07	7.67±0.95
15	1.04±0.06	5.09±0.38	1.04±0.28	2.80±0.30	6.75±0.53	0.22±0.06	3.85±0.64
30	0.67±0.13	3.42±0.68	0.96±0.28	1.36±0.07	4.86±0.08	0.11±0.03	1.56±0.17
60	0.37±0.04	2.37±0.38	0.56±0.11	0.67±0.14	3.06±0.24	0.06±0.00	0.69±0.12

Table 2 Distribution of ^{99m}Tc -MGGQ in mice (%ID/g, n=3)

t/min	Heart	Liver	Spleen	Lung	Kidney	Brain	Blood
0.5	4.70±0.15	6.38±0.89	1.56±0.63	9.81±0.83	12.02±0.64	0.57±0.06	15.80±3.45
2	2.58±0.43	4.48±0.90	1.11±0.53	7.59±1.00	24.77±0.31	0.41±0.11	12.35±1.14
5	2.72±0.21	5.03±0.24	1.36±0.11	6.86±0.32	18.93±1.68	0.33±0.15	10.01±0.58
15	1.12±0.23	3.74±0.48	0.75±0.10	3.14±0.35	7.95±1.63	0.19±0.08	4.38±0.53
30	0.67±0.14	2.32±0.31	0.48±0.04	1.43±0.20	4.02±0.22	0.08±0.01	2.01±0.49
60	0.18±0.02	0.72±0.23	0.15±0.04	0.45±0.21	1.01±0.28	0.03±0.00	0.41±0.07

Table 3 Distribution of ^{99m}Tc -MAGQ in mice (%ID/g, n=3)

t/min	Heart	Liver	Spleen	Lung	Kidney	Brain	Blood
0.5	4.10±0.44	3.24±0.38	2.05±0.50	9.02±1.85	12.99±2.06	0.43±0.23	13.54±0.3
2	2.64±0.32	3.22±0.38	2.13±0.43	6.64±0.62	14.74±0.48	0.29±0.07	8.05±1.07
5	1.93±0.26	3.35±0.52	2.37±0.41	5.05±0.60	12.18±2.12	0.20±0.03	5.72±0.78
15	1.69±0.39	3.06±0.75	1.94±0.15	3.89±0.75	8.23±1.23	0.16±0.04	3.94±0.97
30	1.08±0.09	2.77±0.41	1.58±0.46	2.37±0.22	5.34±0.49	0.10±0.02	2.49±0.12
60	0.71±0.13	2.66±0.29	1.18±0.18	1.69±0.08	4.39±0.17	0.08±0.01	1.69±0.16

Table 4 Distribution of ^{99m}Tc -MVGQ in mice (%ID/g, n=3)

t/min	Heart	Liver	Spleen	Lung	Kidney	Brain	Blood
0.5	4.40±0.74	10.55±3.45	2.74±0.93	10.19±1.54	41.57±6.22	0.50±0.05	18.69±3.12
2	3.06±0.48	16.45±3.12	2.63±0.17	7.37±0.88	43.66±6.11	0.45±0.11	10.49±1.55
5	1.54±0.04	17.51±0.51	2.12±0.3	3.45±0.67	28.14±1.12	0.26±0.03	4.90±0.33
15	0.66±0.06	7.79±1.21	1.40±0.41	1.34±0.53	9.64±0.08	0.14±0.02	2.01±0.26
30	1.05±0.35	4.03±0.51	2.47±0.63	2.57±0.57	4.94±0.82	0.18±0.04	2.07±0.34
60	0.60±0.12	3.13±0.38	1.14±0.26	1.88±0.23	2.64±0.28	0.09±0.02	2.26±0.33

Table 5 Distribution of ^{99m}Tc - MFGQ in mice (%ID/g, n=3)

t/min	Heart	Liver	Spleen	Lung	Kidney	Brain	Blood
0.5	6.22 \pm 1.15	14.00 \pm 3.01	3.17 \pm 1.25	15.72 \pm 1.62	19.23 \pm 2.73	0.63 \pm 0.09	22.87 \pm 4.21
2	3.30 \pm 0.42	17.60 \pm 2.36	2.18 \pm 0.62	8.71 \pm 1.38	22.31 \pm 2.75	0.24 \pm 0.03	8.25 \pm 1.23
5	2.25 \pm 0.35	13.91 \pm 1.28	2.59 \pm 0.49	4.26 \pm 0.35	8.96 \pm 1.30	0.22 \pm 0.06	5.78 \pm 0.28
15	1.04 \pm 0.02	5.55 \pm 0.57	1.54 \pm 0.29	2.38 \pm 0.21	4.84 \pm 0.38	0.23 \pm 0.10	2.67 \pm 0.18
30	0.98 \pm 0.09	5.86 \pm 1.06	1.70 \pm 0.22	1.88 \pm 0.15	4.68 \pm 0.48	0.13 \pm 0.04	2.07 \pm 0.21
60	0.76 \pm 0.09	5.85 \pm 1.11	1.70 \pm 0.51	1.46 \pm 0.21	4.36 \pm 0.54	0.07 \pm 0.03	1.73 \pm 0.22

Table 6 Activity ratios of kidneys to other tissues of ^{99m}Tc -MGGQ

T/min	0.5	2	5	15	30	60
$A_{\text{kidney}}/A_{\text{blood}}$	0.76	2.01	1.89	1.82	2.00	2.48
$A_{\text{kidney}}/A_{\text{liver}}$	1.88	5.53	3.76	2.12	1.73	1.39
$A_{\text{kidney}}/A_{\text{lung}}$	1.23	3.26	2.76	2.53	2.81	2.31

Table 7 Activity ratios of kidneys to other tissues of ^{99m}Tc -MVGQ

T/min	0.5	2	5	15	30	60
$A_{\text{kidney}}/A_{\text{blood}}$	2.22	4.16	5.75	4.80	1.20	1.17
$A_{\text{kidney}}/A_{\text{liver}}$	3.94	2.65	1.61	1.24	1.22	0.84
$A_{\text{kidney}}/A_{\text{lung}}$	4.08	5.92	8.15	7.19	1.92	1.40

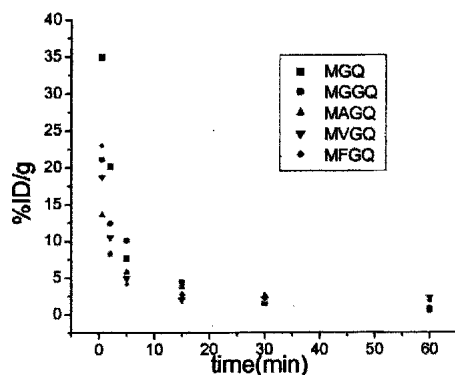


Fig. 1. Blood clearance curves of the compounds

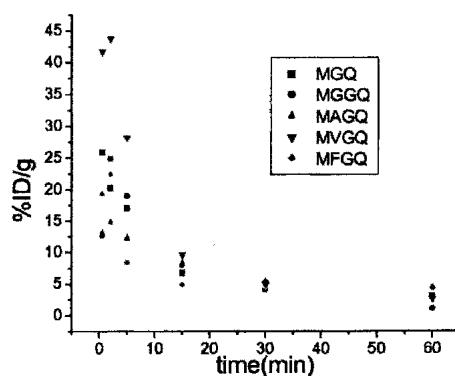


Fig. 2. Renal clearance curves of the compounds

Computational Studies

In order to obtain as much useful information as possible, quantum-chemical calculations of the series of complexes studied were performed on a PC computer using Hyperchem software for windows (Version 7.0). Besides the complexes we synthesized in this study, we also cited other molecules in order to form a more complete dataset. The initial molecular structures were produced by Model Build Module and further optimized under Gaussian 98 using the method of B3LYP/LANL2DZ. The generated molecular conformations were then optimized by a semi-empirical quantum mechanics method ZINDO/1. A series of descriptors of quantum mechanics were then obtained.

Of all the descriptors, there were six electronic parameters, including the energy of the lowest unoccupied molecular orbital (E_{lumo}) and the highest occupied molecular orbital (E_{homo}), the maximum positive atomic charge ($Q^{+\text{max}}$), the maximum negative atomic charge ($Q^{-\text{max}}$), the sum of all positive atomic charges (ΣQ^+) and the dipole moment (μ). In addition, four steric parameters including molecular polarization (P), molecular volume (V), molecular refraction (MR) and molecular surface area (SAG), and the lipophilic parameter logP was also calculated. In addition to all the descriptors obtained through calculation, the indicative variable I_0 was also introduced, which equaled 1 when the molecular charge was -2 , and 0 for other valances.

Calculations of molecular volume, polarization, dipole moment, refraction and surface area were also carried out using the Hyperchem (7.0) software and the Quantitative Structure Activity Relationships Properties Module. Net charges of all atoms, E_{lumo} and E_{homo} , were calculated by the ZINDO/1 method.

Based on the results of the above calculations, correlation of kidney uptake values with obtained parameters and regression analysis of the QSAR study were performed using a standard program (GFA BASIC 4.38) on a PC computer. Multiple regression

analyses which involved finding the best fit of dependent variables (kidney uptake values $\log (\%ID/g)$) to a linear combination of independent variables (descriptors) employed the least squares method. Stepwise regression analysis was used to determine the most significant descriptors. For each regression, the following descriptive information was provided: the number of data points used to derive regression equation (n), the correlation coefficient (r), the standard error of the estimate (s), the value of F-test (F) and the cross-validated correlation coefficient ($r_{cr.val.}$) derived from the predictive residual sum of squares (leave-one-out method). The “leave-one-out” procedure was used to determine the predictive ability of the mathematical model proposed. In this procedure, one compound was removed from the data set, and the correlation equation was established from the remaining compounds and used to predict the discarded compound. The process was repeated in turn for each compound in the data set. All the coefficients were given with 95% intervals. The results obtained from the above regimen are presented below:

Table8 Renal uptake value (ID/g) and corresponding descriptors

	%ID	log%ID	Q^{max}	E_{homo}	I_0
MAGQ	14.74	1.168	-0.6257	0.02698	1
MGQ	20.29	1.307	-0.6196	0.03761	1
MGGQ	24.77	1.394	-0.6204	0.02684	1
MFGQ	22.31	1.348	-0.6201	0.0272	1
MVGQ	43.66	1.64	-0.6149	0.02627	1
MGN	57.38	1.759	-0.6142	0.04025	1
MVN	42.56	1.629	-0.6119	0.03116	1
MPGG	28.96	1.462	-0.6312	0.04297	1
MPGH	12.27	1.089	-0.4852	-0.1229	0
MPGT	13.84	1.141	-0.4594	-0.11992	0
MPNM	9.33	0.97	-0.4063	-0.22937	0
MPNE	4.14	0.617	-0.4078	-0.22792	0
MVGG	30.56	1.485	-0.6324	0.04641	1
MVGH	6.67	0.824	-0.4893	-0.11777	0
MVGT	7.57	0.879	-0.464	-0.1105	0
MVNM	7.08	0.85	-0.4071	-0.23698	0
MVNE	5.98	0.777	-0.4074	-0.23543	0

Using the above data, the following equations were established:

$$\log(\%ID/g) = -0.447(\pm 0.538) - 0.306(\pm 0.988)Q^{-max}$$

$$n=17, \quad s=0.178, \quad r = 0.863, \quad F = 43.64, \quad r(cr.val.) = 0.822 \quad (1)$$

$$\log(\%ID/g) = 0.893(\pm 0.135) + 0.572(\pm 0.185)I_0$$

$$n=17, \quad s = 0.179, \quad r = 0.862, \quad F = 43.50, \quad r(cr.val.) = 0.819 \quad (2)$$

$$\log(\%ID/g) = 1.363(\pm 0.103) + 2.589(\pm 0.797)E_{HOMO}$$

$$n=17, \quad s = 0.172, \quad r = 0.873, \quad F = 47.93, \quad r(cr.val.) = 0.835 \quad (3)$$

Equations (1), (2), (3) reveal that the logarithm of the renal initial uptake ($\log(\%ID/g)$) correlates well with Q^{-max} , I_0 and E_{HOMO} , demonstrating good correlation.

In Eq. (1), the Q^{-max} well correlates negatively with renal uptake. This might be explained by the fact that the filtration barrier system in the kidney possesses negative charges, which may be the determining factor in this system¹⁹. The lower the Q^{-max} , the more easily the complex is “trapped” in the kidney because of the electrostatic attraction to the glomerulus.

In Eq. (2), the indicative variable I_0 has a positive correlation with the renal initial uptake value. Of our series of complexes, there are two valences, -1 and -2. I_0 equals to 1 when the valence is -2, and 0 when -1. Eq. (2) indicate that the complex's valence is very important to renal uptake and the complexes with -2 valence would have better renal initial uptake. The cause may be due to the enhancing of the total negative charges, which improved the hydrophilicity of the complexes and, in turn this, to a certain extent, improved renal uptake.

Eq.(3) reveals that E_{HOMO} correlates positively with renal uptake. It might be explained that higher E_{HOMO} contributes to better hydrophilicity and concomitantly to better renal uptake.

Other parameters such as ΣQ^+ , μ , MR etc., didn't show a correlation with the renal initial uptake value.

Based on this aspect of the study, it appears that the renal uptake value is improved when the total valence of complexes is -2 than -1 . A lower Q^{max} may exert a positive influence.

Conclusion

Five target chelators have been synthesized, characterized and evaluated as renal imaging agents. From investigations of their biological activities in mice, we identified ^{99m}Tc -MGGQ, as a potential candidate for a renal dynamic imaging agent. ^{99m}Tc -MVGQ is also a promising candidate, but it still needs some synthetic improvement. Although fairly good results have been obtained, further research needs to be carried out to obtain even better target compounds.

Experimental Section

Protection of the mercapto group

In a 50mL single -necked flask, redistilled mercapto acetic acid (0.01mol), a mixed solution of dichloromethane (3mL) and glacial acetic acid (3mL), and TrCl (Trityl chloride) (0.01mol) were added and stirred thoroughly, followed by addition of $\text{BF}_3 \cdot \text{Et}_2\text{O}$ (2mL). The mixed solution was stirred for 1h at room temperature and a precipitate formed. After the CH_2Cl_2 was evaporated under reduced pressure, 10mL H_2O was added to the residue to remove $\text{BF}_3 \cdot \text{Et}_2\text{O}$. The solids, collected by filtration, were washed with water ($3 \times 10\text{mL}$), CH_3CN (5mL), and glacial ethyl ether (2mL), respectively, to obtain 3.1g of product (93% yield). The product was purified via recrystallization in benzene to provide colorless crystals.

Preparation of active ester of compounds 2, .4, 5, 6 and 7

To 4 mmol of DCC dissolved in 3 mL anhydrous THF was added 4 mmol of 2 and 4

mmol of NHS in 4 mL anhydrous THF. The reaction was maintained at -5°C for 2h, and then the mixture was stirred at room temperature for 16 h. The filtrate was evaporated to dryness and recrystallized in ethyl acetate.

Synthesis of compounds 4, 5, 6 and 7

To 4 mmol of amino acid dissolved in 0.2 M NaOH solution was added 4 mmol active ester 3 in 80 mL acetonitrile in a 250 mL three-necked flask equipped with a condenser, stirrer and reacted at $40\text{--}50^{\circ}\text{C}$. The reaction was maintained at this temperature for 2h when TLC showed that the starting material had disappeared. Then the reaction was stopped. The pH of the solution was adjusted to 1 with dilute H_2SO_4 in an ice bath. A white precipitate was formed and filtrated without further purification.

Synthesis of target ligands

To 4 mmol of amino acid dissolved in 0.2 M NaOH solution was added 4 mmol active ester 3 in 80 mL acetonitrile in a 250 mL three-necked flask equipped with a condenser, stirrer and reacted at $40\text{--}50^{\circ}\text{C}$ for 2h. When TLC showed that the starting material had disappeared, the reaction was stopped. The pH was adjusted to 1 with dilute H_2SO_4 in an ice bath. The solution was cloudy. This was extracted with ethyl acetate, the target compounds in the organic layer were dried with anhydrous magnesium sulfate, then purified by column chromatography using dichloromethane/methanol (10:1) as the eluent in the presence of 1% triethylamine, in order to prevent decomposition. A white powder was obtained.

Biological studies

Deprotection of compounds

Target compounds (5.11×10^{-5} mol) and TFA (3mL) were added to a 10mL flask. After the reaction mixture was stirred at room temperature for 5 min, HSiEt_3 (1mL) was added and stirring continued for 5 min. Most of the TFA was evaporated off and 4mL 0.1M NaOH or 4mL 0.1M HCl was added to the residue. By extracting with

dichloromethane (5mL), the triphenylmethane in the organic layer was removed. The water layer was protected by nitrogen, followed by labeling with Tc-99m.

Radiochemical analysis

Polyamide and filter paper strips were developed in 0.9% aqueous NaCl. To about 7cm from the origin and cut into 10 equal segments. The radioactivity on each segment was measured and expressed as the percent of total activity on the strips. For example, R_f values of $^{99m}\text{TcO}_4^-$, $^{99m}\text{TcO}_2 \cdot 2\text{H}_2\text{O}$, $^{99m}\text{Tc-MVGQ}$ were 0.1, 0.1, 1.0(on polyamide) and 0.8,0.1,1.0(on filter paper), respectively. Radiochemical purities were typically higher than 93%.

Acknowledgments

We wish to express our appreciation to the Returnee Fund of the Ministry of Education of the People's Republic of China and also the open fund support of Liaoning key Laboratory of Bio-organic Chemistry.

Reference

1. Fritzberg A.R; Kasina S; Eshima D. *J.Nucl. Med.* **1986**, 27, 111-116.
2. Liu,S.; Scott, D.E. *Chem. Rev.* **1999**, 99, 2235-2268.
3. Okarvi, S.M. *Nuclear Medicine Communications.* **1999**, 20, 1093-1112.
4. Virgoline, T. T.; Novotny, C.; Leimer, M.; FÜGER, B.; Li, S. R.; Patri, P.; Pangerl,T.; Angelberger, P.; Raderer, M.; Andreae,F.; Kurtaran,A.; Dudczak,R. *Q. J. NUCL. MED.* **2001**, 45, 153-159.
5. Signore, A.; Annovazzi, A.; Chianelli, M.; Corsetti, F.; Van de Wiele, C.; Watherhouse, R. N.; Scopinaro, F. *Eur. J. Nucl. Med.* **2001**, 28, 1555-1565.
6. Barrett, J. A.; Damphousse, D. J.; Heminway, S. J. *Bioconj. Chem.* **1996**, 7, 203-208.
7. Pearson, D.A.; Lister-James, J.; McBride, W. J. *J. Med. Chem.* **1996**, 39, 1372-1382.

8. Richard, R. P.; Thomas, M. *Seminars in Nuclear Medicine*. **2002**, Vol.XXXIII, 2, 79-83.
9. García-Garayoa, E.; Bläuenstein, P.; Bruehlmeier, Matthias.; Blanc, Alain.; Iterbeke, Koen.; Conrath, Peter.; Tourwé, D.; Schubiger, P.A. *J. Nucl. Med.* **2002**, *43*, 374-383.
10. Volkert, W.A.; Hoffman, T.J.; Seger, R.M.; Troutner, D.E.; Holmes, R.A. *Eur. J. Nucl. Med.* **1984**, *9*, 511-521.
11. Cheesman, E.H.; Blanchette, M.A.; Ganey, M.V.; Mahen, L.J.; Wheless, J. *J. Nucl. Med.* **1988**, *29*, 788-795.
12. Hubert, P.; Vanbilloen, B. J.; Alfons, M. V. *Nuclear Medicine & Biology*. **2000**, *27*, 207-214.
13. Mang'era, K.O.; Tassawet, S.; Cleynhens, B.; Verbruggen, A.; Verbeke, K. *J. Labelled Cpd. Radiopharma.*, **2001**, *44*, 257-264.
14. Lipowska, M.; Hansen, L.; Xu, X. L.; Marzilli, P. A.; Taylor, A.; Marzilli, L. G. *Inorg. Chem.* **2002**, *41*, 3032-3041.
15. Zhang, H.B.; Dai, M.; Qi, C.M.; Li, B.; Guo, X. F. *Applied radiation and Isotopes*. **2004**, *60*, 643-651.
16. Qi, C.M.; Yang, L.C.; Zhang, H.B.; Guo, X.F.; Feng, S.J., Li, B. *Med. Chem. Res.* **2002**, *11*, 345-359.
17. Capretta A.; Rabindranath B.; Russell A.B. *Carbohydrate Res.* **1995**, *267*, 49-63.
18. Schneider, R.F.; Subramanian, G.; Feld, T.A.; McAfee, J.G.; Zapf-Longo, C.; Palladino, E.; Thomas, F.D. *J. Nucl. Med.*. **1984**, *25*, 223-229.
19. Andrew, T.; Dennis, E.; Alan R.F.; Paul, E.C.; Sudhakar, K. *Renal Imaging Volunteers*. **1986**, *27*, 795-803.

Received: 9-21-04 Accepted: 4-15-05